NEOPLASIA
www.neoplasia.com

Volume 20 Number 7 July 2018 pp. 668–677 668

Biologic Response of Colorectal Cancer Xenograft Tumors to Sequential Treatment with Panitumumab and Bevacizumab

Hiroya Taniguchi[*,1], Yuji Baba[†,1], Yoji Sagiya[‡], Masamitsu Gotou[†], Kazuhide Nakamura[†], Hiroshi Sawada[†], Kazunori Yamanaka[†], Yukiko Sakakibara[‡], Ikuo Mori[‡], Yukiko Hikichi[§], Junpei Soeda[‡] and Hideo Baba[‖]

[*]Department of Clinical Oncology, Aichi Cancer Center Hospital, Nagoya 464-8681, Japan.; [†]Pharmaceutical Research Division, Takeda Pharmaceutical Company Limited, Fujisawa, Kanagawa 251-8555, Japan; [‡]Japan Medical Affairs, Japan Oncology Business Unit, Takeda Pharmaceutical Company Limited, Tokyo 103-8668, Japan; [§]Product Information Group, Japan Oncology Business Unit, Takeda Pharmaceutical Company Limited, Tokyo 103-8668, Japan; [‖]Department of Gastroenterological Surgery, Kumamoto University, Kumamoto 860-8556, Japan

Abstract

Recent studies in *RAS* wild-type (WT) metastatic colorectal cancer (mCRC) suggest that the survival benefits of therapy using anti-epidermal growth factor receptor (anti-EGFR) and anti-vascular endothelial growth factor (anti-VEGF) antibodies combined with chemotherapy are maximized when the anti-EGFR antibody is given as first-line, followed by subsequent anti-VEGF antibody therapy. We report reverse-translational research using LIM1215 xenografts of *RAS* WT mCRC to elucidate the biologic mechanisms underlying this clinical observation. Sequential administration of panitumumab then bevacizumab (PB) demonstrated a stronger tendency to inhibit tumor growth than bevacizumab then panitumumab (BP). Cell proliferation was reduced significantly with PB ($P < .01$) but not with BP based on Ki-67 index. Phosphoproteomic analysis demonstrated reduced phosphorylation of EGFR and EPHA2 with PB and BP compared with control. Western blotting showed reduced EPHA2 expression and S897-phosphorylation with PB; RSK phosphorylation was largely unaffected by PB but increased significantly with BP. In quantitative real-time PCR analyses, PB significantly reduced the expression of both lipogenic (*FASN, MVD*) and hypoxia-related (*CA9, TGFBI*) genes versus control. These results suggest that numerous mechanisms at the levels of gene expression, protein expression, and protein phosphorylation may explain the improved clinical activity of PB over BP in patients with *RAS* WT mCRC.

Neoplasia (2018) 20, 668–677

Abbreviations: BB, bevacizumab-bevacizumab; BP, bevacizumab followed by panitumumab; CA9, carbonic anhydrase 9; CRC, colorectal cancer; DEGs, differentially expressed genes; EGFR, epidermal growth factor receptor; EPHA2, ephrin type-A receptor 2; FASN, fatty acid synthase; FOLFIRI, fluorouracil, leucovorin, and irinotecan; FOLFOX, fluorouracil, leucovorin, and oxaliplatin; GR, growth rate; GTPase, guanosine triphosphate hydrolase; HIF, hypoxia-inducible factor; HMGCR, HMG-CoA reductase; HR, hazard ratio; IGF2R, insulin-like growth factor 2 receptor; LSS, lanosterol synthase; MAPK, mitogen-activated protein kinase; mCRC, metastatic colorectal cancer; MVD, mevalonate disphosphate decarboxylase; OS, overall survival; PB, panitumumab followed by bevacizumab; pEPHA2, phosphorylated EPHA2; PFS, progression-free survival; pRSK, phosphorylated RSK; qRT-PCR, quantitative real-time polymerase chain reaction; RSK, ribosomal S6 kinase; SCID, C.B17/Icr-scid/scid Jcl; SDS, sodium dodecyl sulfate; TGFBI, transforming growth factor-β induced protein; VEGF, vascular endothelial growth factor; WT, wild-type

Address all correspondence to: Junpei Soeda, MD, PhD, Japan Medical Affairs, Japan Oncology Business Unit, Takeda Pharmaceutical Company Limited, 12-10 Nihonbashi 2-chome, Chuo-ku, Tokyo 103-8668, Japan.
E-mail: jumpei.soeda@takeda.com
[1]These authors have contributed equally to the work.
Received 27 March 2018; Revised 24 April 2018; Accepted 24 April 2018

1476-5586/18
https://doi.org/10.1016/j.neo.2018.04.006

Introduction

Colorectal cancer (CRC) is the third most common cancer in men and the second most common in women, accounting for approximately 1.36 million new cases and 694,000 deaths worldwide each year [1]. Approximately 25% of CRC patients present metastatic disease (mCRC) at diagnosis, and almost half will subsequently develop metastases [2]. The current standard of care for mCRC involves a backbone of cytotoxic chemotherapy, using regimens such as FOLFIRI (fluorouracil, leucovorin, and irinotecan) and FOLFOX (fluorouracil, leucovorin, and oxaliplatin) combined with targeted agents [2,3]. Such regimens involving an anti-epidermal growth factor receptor (EGFR) antibody, such as panitumumab and cetuximab, or the anti-vascular endothelial growth factor (VEGF) antibody, bevacizumab, in combination with chemotherapy, improve survival compared with chemotherapy alone [4–9].

RAS is a small guanosine triphosphate hydrolase that is constitutively activated by mutation in ~20% of human cancers [10]. *KRAS* is the predominantly mutated isoform in CRC [10]; 55.9% of patients with CRC harbor a *RAS* (*KRAS/NRAS*) mutation [11]. Constitutive RAS activation facilitates oncogenesis through the up-regulation of signaling pathways such as mitogen-activated protein kinase (MAPK) and Akt [12,13].

Potential benefit with anti-EGFR antibodies appears to be limited to patients with *RAS* wild-type (WT) mCRC [14–16]; such patients had improved clinical outcomes when treated with an anti-EGFR antibody and chemotherapy as first-line therapy than when compared with an anti-VEGF antibody and chemotherapy [17]. *Post-hoc* analysis of the FIRE-3 study, in which patients with *RAS* WT mCRC received treatment with FOLFIRI plus cetuximab or bevacizumab, highlighted a durable overall survival (OS) advantage for the group of patients that received FOLFIRI and cetuximab as first-line therapy compared with FOLFIRI and bevacizumab (median 33.1 vs. 25.0 months; hazard ratio [HR] 0.70; $P = .0059$) [17]. There have also been indications that first-line therapy in *RAS* WT mCRC can determine the efficacy of subsequent treatments and affect outcomes [18–20]. Furthermore, an exploratory analysis of data from three randomized studies of mCRC suggested a trend towards improved OS with a first-line anti-EGFR antibody plus chemotherapy followed by a second-line anti-VEGF antibody compared with the opposite sequence [21].

While the use of an anti-EGFR antibody in first-line treatment can increase the efficacy of second-line anti-VEGF antibodies [22,23], initial treatment with an anti-VEGF antibody may decrease the efficacy of subsequent anti-EGFR antibodies [24–26]; a sufficient anti-VEGF antibody-free period prior to treatment with second-line anti-EGFR antibodies is necessary to limit this reduced efficacy [27]. The biologic rationale for this finding remains unknown, but mechanisms have been suggested that may contribute [19,20]. *RAS* WT mCRC tumor cells that develop resistance to an anti-EGFR antibody may retain sensitivity to an anti-VEGF antibody, but resistance to an anti-VEGF antibody can lead to the development of resistance to anti-EGFR antibodies [19,20]. Indirect evidence for this comes from the finding that resected liver metastases from Japanese patients with mCRC treated with bevacizumab demonstrated significantly increased tumoral *VEGFA* mRNA expression [28], while in pre-clinical models of CRC, overexpression of *VEGFA* or treatment with exogenous VEGF-A ligand conferred resistance to cetuximab [24,29]. Taken together, these findings highlight a potential mechanism of acquired resistance to anti-EGFR antibodies in mCRC that potentiates tumor angiogenic ability. Nevertheless, many details regarding the biologic mechanisms underlying the efficacy of the two different treatment sequences in the clinic are yet to be explored.

Here, we present the results of reverse-translational research using xenograft models of human CRC to evaluate the biologic reasons for the improved outcomes seen with sequential use of an anti-EGFR antibody (panitumumab) followed by an anti-VEGF antibody (bevacizumab) compared with the opposite sequence in patients with *RAS* WT mCRC. We performed quantitative phosphoproteomic and transcriptome analyses of xenograft tumors to identify biological changes with sequential treatment that may provide some explanation for the survival benefits previously demonstrated in clinical settings.

Materials and Methods

Cells and Reagents

The human colon cancer cell line LIM1215 was obtained from the European Collection of Authenticated Cell Cultures (ECACC, Salisbury, UK). LIM1215 cells were cultured in conditions recommended by the ECACC. Panitumumab was provided by Amgen (Thousand Oaks, CA, USA). Bevacizumab was purchased from Roche (Basel, Switzerland).

Xenograft Construction and Study Treatment

All in vivo experimental protocols complied with the Guide for the Care and Use of Laboratory Animals (8th Edition), and were approved by the Institutional Animal Care and Use Committee of the Shonan Research Center (#00011823), Takeda Pharmaceutical Company Limited, or Shanghai Medicilon Inc. (Shanghai, China).

LIM1215 cells were selected because they have WT *RAS (*WT *KRAS* and *NRAS)* and WT *BRAF*, and panitumumab and bevacizumab have previously shown anti-tumor effects in xenografts of LIM1215 tumors [30]. Six- to seven-week-old female C.B17/Icr-scid/scid Jcl (SCID) mice (from CLEA, Tokyo, Japan, or Beijing Vital River Animal Technology, Beijing, China) maintained under specific pathogen-free conditions were injected subcutaneously in the right flank with 5 million LIM1215 cells mixed with Matrigel (Corning, NY, USA). In vivo LIM1215 xenografts were constructed at two different sites, LIM1215(A) and LIM1215(B). Once tumor volume reached 50–200 mm^3, mice were randomized to each treatment group. All treatment was intraperitoneal. The vehicle control group received saline twice-weekly for 2 weeks or 4 weeks. Panitumumab and bevacizumab were given twice-weekly at 3 mg/kg and 10 mg/kg, respectively. The panitumumab-bevacizumab (PB) group received panitumumab for 2 weeks followed by bevacizumab for 2 weeks; the bevacizumab-panitumumab (BP) group received the reverse sequence. One group received bevacizumab (BB) for 4 weeks and other groups received monotherapy with panitumumab (P group) or bevacizumab (B group) for 2 weeks (Supplementary Figure S1).

Tumor volumes (length × $width^2$ × 0.5) were measured twice-weekly with Vernier calipers and antitumor activity was evaluated by percentage of relative growth rate (GR) calculated using the following equation: %GR = (mean growth rate of treated tumor/mean growth rate of vehicle control group) × 100. Following final tumor volume measurements, mice were anesthetized 24 hours after final drug administration and euthanized by cervical dislocation, and tumor samples were collected. Samples from the LIM1215(A) xenografts were used for the transcriptome and phosphoproteome analyses, and quantitative real-time PCR (qRT-PCR). The LIM1215(B) xenograft samples were used for qRT-PCR, western blotting, and histology analyses.

Tumor Tissue Analyses

Formalin-fixed paraffin-embedded sections (4 μm) of resected tumor tissue were used for histologic analysis. Hematoxylin and eosin staining

was conducted according to standard protocol. Ki-67 staining was performed with anti-Ki-67 antibody (Nichirei Biosciences, Tokyo, Japan) and hematoxylin background. The Ki-67 index (%) was estimated by counting the number of Ki-67-positive cell nuclei per 1200–1800 tumor cells in the three regions of the tumor with the greatest staining density.

Phosphoproteomic Analysis and Western Blotting

Quantitative phosphoproteomic analysis of xenografts was performed using mTRAQ technology (AB Sciex, Framingham, MA, USA). Xenografts were homogenized in homogenization buffer (10 mM phosphate [pH 7.5], 8 M urea, protease inhibitor, and phosphatase inhibitors) and proteins were precipitated with 5 volumes of acetone followed by resolution in lysis buffer (4% sodium dodecyl sulfate [SDS, SERVA Electrophoresis GmbH, Heidelberg, Germany], 0.4% 3-[3-cholamidopropyl] dimethylammoniopropanesulfonate [CHAPS, DOJINDO, Kumamoto, Japan] and 10 mM triethylammonium bicarbonate [TEAB, Wako, Osaka, Japan]). Each lysate, and a mixture of all lysates (internal standard), were digested with Lys-C (Wako, Osaka, Japan) and trypsin (Promega, Madison, WI, USA) by the FASP method [31] using Amicon Ultra-4 30 k centrifugal filter units (Merck KGaA, Darmstadt, Germany). The digested peptides were loaded onto TiO_2 chips (GL Science, Tokyo, Japan) for phosphopeptide enrichment, and phosphopeptides were labeled with mTRAQ reagent (AB Sciex, Framingham, MA, USA). Labeled phosphopeptides from each sample and the internal standard were mixed and separated into 12 fractions on a polysulfoethyl A SCX column (PolyLC, Columbia, MD, USA). The fractions were then analyzed using fusion mass spectrometry (MS) (Thermo Scientific, Waltham, MA, USA) coupled to a nano-liquid chromatography system (EASY-nLC 1000). MS files were processed with Proteome Discoverer 1.4 (Thermo Scientific, Waltham, MA, USA) using MASCOT (v. 2.5, Matrix Science, London, UK). The ratio of sample:vehicle was calculated by sample:mixture / vehicle:mixture.

For western blotting, RIPA buffer (Wako, Osaka, Japan) containing inhibitors (#78443, Thermo Scientific, Waltham, MA, USA) was added to the recovered tumor, and lysis was carried out using a bead homogenizer. The protein concentration of the supernatant was measured by BCA Protein Assay (Bio-Rad, Hercules, CA, USA). Tissue lysates were subjected to SDS-polyacrylamide gel electrophoresis (SDS-PAGE, Criterion TGX precast gels, Bio-Rad, Hercules, CA, USA) and transfer by Trans-Blot Turbo System (Bio-Rad, Hercules, CA, USA). Antibodies used were as follows: anti-ephrin type-A receptor 2 (EPHA2; #6997), anti-phospho-EPHA2 (S897; #6347), anti-ribosomal S6 kinase (RSK) (#8408), anti-phospho-RSK (S380; #11989), and anti-β-actin (#5125) (all from Cell Signaling Technology, Danvers, MA, USA). Western blots were developed using ImmunoStar Zeta or ImmunoStar LD (Wako, Osaka, Japan). Band densities were quantified by an image analyzer (LAS-3000, Fujifilm, Tokyo, Japan).

Transcriptome Analysis and qRT-PCR

Total RNA was extracted from tumor tissue and treated with DNase using the RNeasy Mini Kit (QIAGEN, Germantown, MD, USA) according to the manufacturer's recommendations. Gene expression analysis was conducted by microarray on SurePrint G3 Human GE 8X60k V3 Microarrays (Agilent, Santa Clara, CA, USA) according to the manufacturer's guidelines. Signal values were logarithmically transformed and subjected to quantile normalization. Statistical significance of the expression data was determined using fold change (above 1.5 fold) and independent *t*-test (*P*-value < .05) between two groups in array probes with Flag-P in both groups. Sets of differentially expressed genes (DEGs) were selected using the Omicsoft Array Studio (QIAGEN, Germantown, MD, USA). Enrichment analysis for DEG sets (Diseases and Bio Functions, Canonical Pathways) was performed using Ingenuity Pathway Analysis (QIAGEN, Germantown, MD, USA).

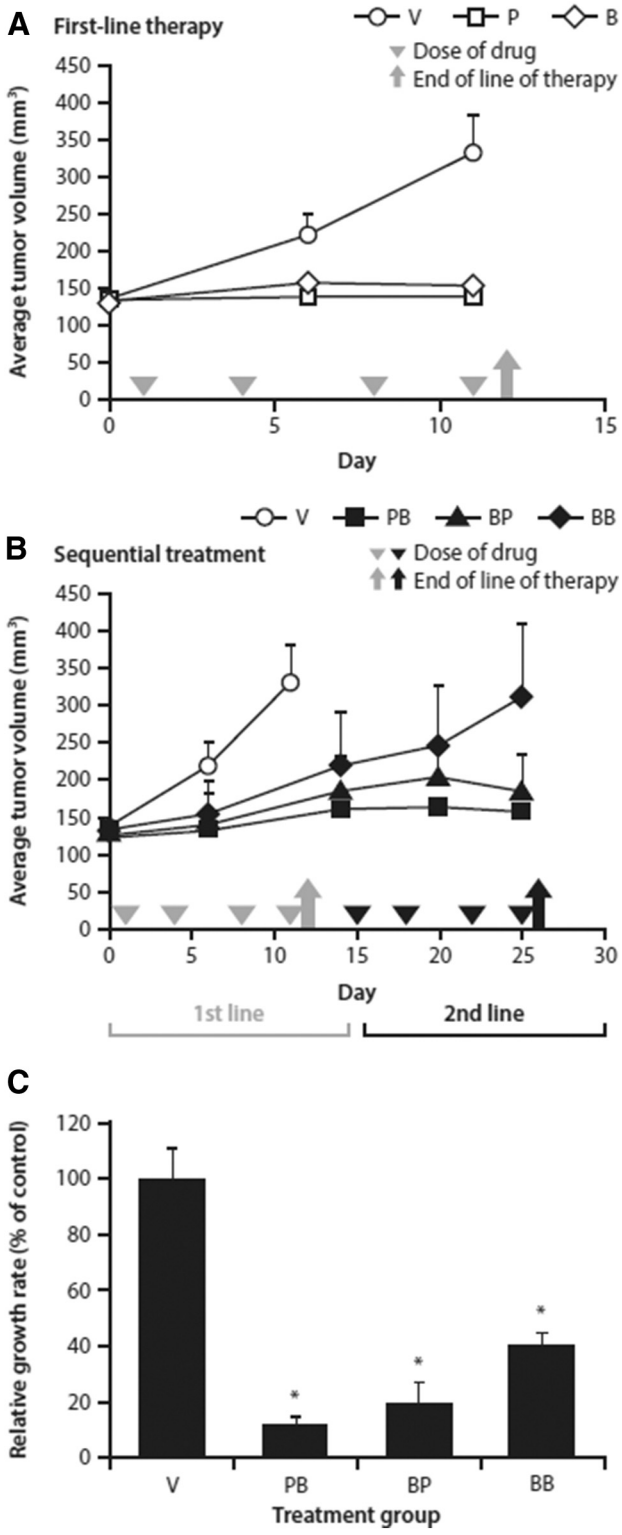

Figure 1. Antitumor effect in LIM1215(A) xenografts by treatment received. (A and B) assessed by average tumor volume and (C) relative growth rate. Arrowheads indicate dosing. Arrows indicate sample harvesting. Data represent mean ± SE. (n = 3–7. *P < .05). B, bevacizumab; P, panitumumab; V, vehicle control.

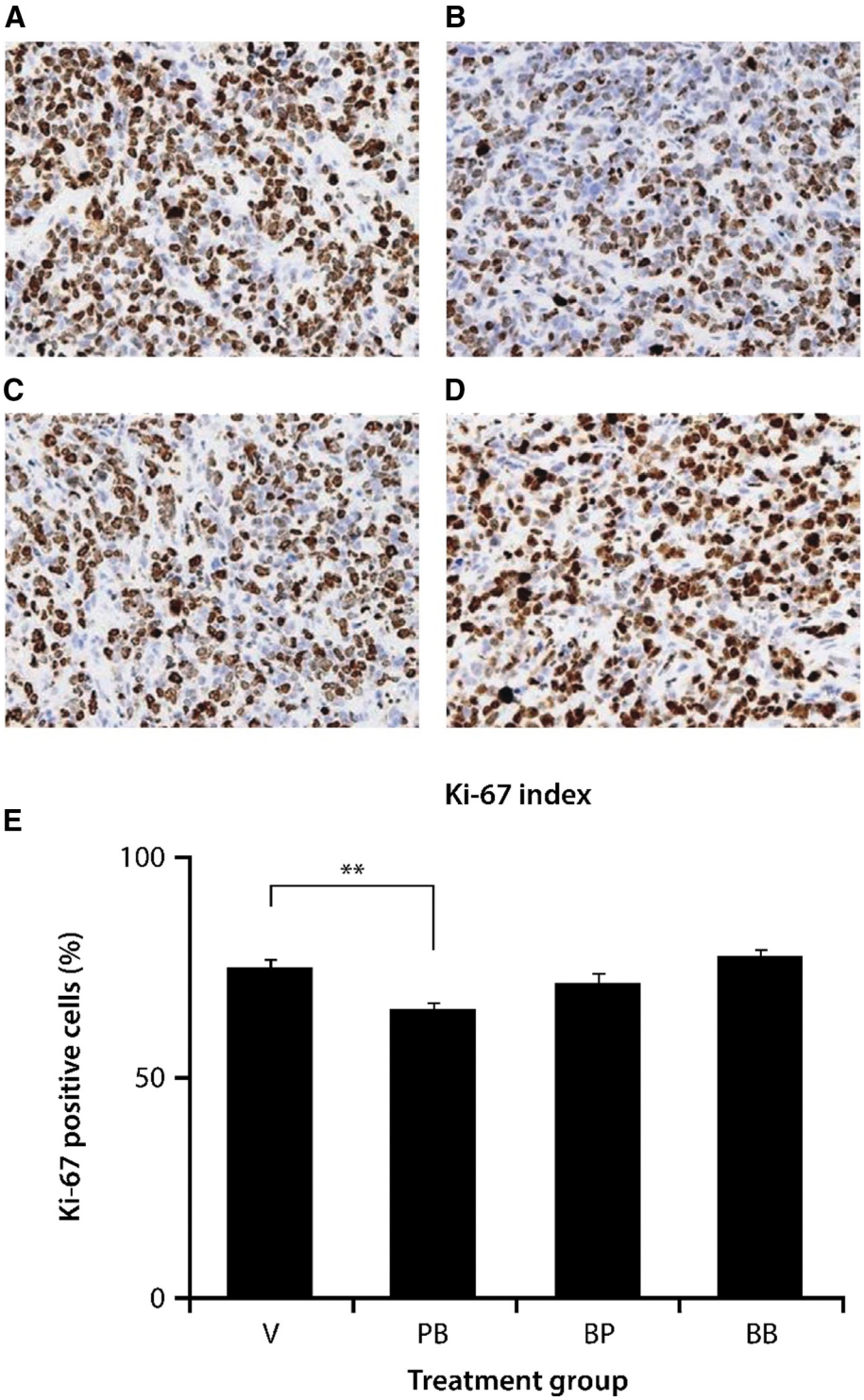

Figure 2. Outcome of immunohistochemistry for Ki-67 in LIM1215(B) xenograft sections. (A) Using vehicle control, (B) panitumumab-bevacizumab, (C) bevacizumab-panitumumab, and (D) bevacizumab-bevacizumab. (E) Proportion of Ki-67-positive cells in all treatment groups. Sections were IHC stained for Ki-67 (brown) and counterstained with hematoxylin (purple). Representative images of the sections are shown. Data in the graph represent the mean ± SE (n = 6–8). $^{**}P < .01$. B, bevacizumab; P, panitumumab; V, vehicle control.

Purified RNA was reverse-transcribed with the High-Capacity cDNA Reverse Transcription Kit with RNase Inhibitor (Thermo Fisher Scientific, Waltham, MA, USA) and qRT-PCR was performed with the TaqMan® Fast Advanced Master Mix (Thermo Fisher Scientific, Waltham, MA, USA) using a ViiA 7 Real-Time PCR System (Thermo Fisher Scientific, Waltham, MA, USA). Relative quantified RNA was normalized to the housekeeping gene β-actin, and results were evaluated using the comparative ΔΔCT method. The TaqMan® Gene Expression Assays (Thermo Fisher Scientific, Waltham, MA, USA) used for each gene are listed in Supplementary Table S1.

Statistical Analyses

Data for vehicle controls and other groups was initially analyzed using Bartlett's test for homogeneity of variance. When variance was

Table 1. Levels of Phosphorylated Growth Factor Receptors in LIM1215(A) Xenografts Treated with PB, BP, and BB Relative to Vehicle Control

Protein Name	Phosphorylation Site	Fold Change vs. Vehicle Control		
		PB	BP	BB
EGFR	pT693 (pT669)	0.60	0.70	1.04
	pS991 (pS967)	0.59	0.71	0.82
	pS1166 (pS1142)	0.81	1.02	0.81
EPHA2	pS897	0.36	0.77	1.07
	pS901	0.42	0.68	1.43
IGF2R	pS2049	0.89	0.84	0.95
	pS2484	1.02	0.91	0.89

B, bevacizumab; P, panitumumab.

homogenous, differences between groups were analyzed by Dunnett's multiple comparison test. When variance was not homogenous, the Steel-Dwass multiple comparison test was used. A significance level of $P < .05$ was used.

Results

PB Was More Effective Than BP at Inhibiting Tumor Growth Rate in Xenograft Models

In the LIM1215(A) xenograft, panitumumab and bevacizumab alone demonstrated almost equivalent efficacy (Figure 1*A*). Obvious growth retardation was observed in all sequential treatment groups (Figure 1*B*). Relative GR was significantly reduced with PB, BP, and BB in LIM1215 (A) xenografts compared with vehicle control and there was a numerically greater decrease in growth rate in the PB group than in the BP group (Figure 1*C*). A significant decrease in relative GR was also apparent in the PB group in LIM1215(B) xenografts (Supplementary Figure S2).

Ki-67 Index Fell with PB

Cell proliferation per Ki-67 index was significantly reduced with PB compared with vehicle controls (66.5% vs. 75.8% Ki-67 positive cells, $P < .01$; Figure 2*E*). Proliferation was also numerically reduced compared with vehicle controls using BP (72.0% Ki-67 positive cells), but to a lesser extent than with PB. The BB treatment sequence did not have an antiproliferative effect (78.1% Ki-67 positive cells) (Figure 2).

EGFR and EPHA2 Phosphorylation Levels Were Reduced with PB and BP

Table 1 shows the phosphopeptides selected from all phosphoproteomic analysis data according to the following criteria: 1, the peptide is a part of growth factor receptor; 2, phosphorylation of the site has previously been identified by a site-specific method (i.e. methods other than omics); 3, signals were detected in all 4 groups (vehicle control, PB, BP, and BB).

Levels of phosphorylated growth factor receptors (EGFR and EPHA2) were reduced with both PB and BP compared with vehicle control (Table 1); changes in insulin-like growth factor 2 receptor were small in all groups. However, PB demonstrated greater reductions in the phosphorylation level of EGFR and EPHA2 than BP. The greatest change was demonstrated for EPHA2 pS897 and EPHA2 pS901; in the PB group, expression was 36% and 42%, respectively, of the level in vehicle controls compared with 77% and 68%, respectively, in the BP group. Treatment with BB did not result in a decrease in the levels of phosphorylated EPHA2 compared with vehicle control, with only slight reductions in phosphorylation of EGFR at S991 and S1166 (Table 1). Further phosphoproteomic data can be found in Supplementary Table S2.

EPHA2 Protein Expression and Ser-897-Phosphorylation Were Decreased by PB, and RSK Phosphorylation Was Increased with BP

EPHA2 was selected for study by western blotting due to its strong inhibition with PB, as demonstrated in phosphoproteomic analysis. Western blotting showed reduction of total EPHA2 protein and EPHA2 S897-phosphorylation (pEPHA2) levels by PB, while BP showed large individual variation; BB had little effect (Figure 3, *A* and *B*). Compared with vehicle controls, the pEPHA2:EPHA2 ratio was reduced significantly with PB ($P < .01$) (Figure 3, *C* and *D*). The pEPHA2:EPHA2 ratio was also reduced with BP, but with less effect than PB (Figure 3*C*).

Due to the known ability of RSK to induce pEPHA2 in a ligand-independent manner [32–34], RSK was also selected for study by western blotting. PB had minimal effect on both levels of total RSK1 protein and RSK S380-phosphorylation (pRSK) compared with vehicle control. Conversely, both BP and BB increased pRSK levels compared with vehicle control (Figure 3, *E* and *F*). The pRSK:RSK ratio was significantly increased by both BP ($P < .001$) and BB ($P < .01$) (Figure 3, *G* and *H*).

Variable Lipogenic Gene Expression Was Observed With Sequential Treatment

Significant changes in pathway activity relating to lipid metabolism occurred in tumors treated with BB (Table 2) and expression levels of some lipogenic genes were higher with BB versus vehicle control (Supplementary Table S3 and S4). Some pathways were changed in the PB and BP groups, and with panitumumab alone, which altered pathways related to lipid metabolism (Supplementary Table S5).

Lipogenic and Hypoxia-Related Gene Expression Was Reduced With PB

qRT-PCR analysis was performed for lipogenic genes based on the results of transcriptome analysis and demonstrated a definite change in lipid metabolism. Significant suppression of the lipogenic genes fatty acid synthase (*FASN*) and mevalonate diphosphate decarboxylase (*MVD*) was demonstrated with treatment using panitumumab alone, but no suppression was apparent with bevacizumab alone (Figure 4, *A* and *C*). Furthermore, expression levels of *FASN* (59% of expression vs. control, $P < .01$) and *MVD* (56% of expression vs. control, $P < .05$) were significantly decreased in the PB group compared vehicle controls, and 3-hydroxy-3-methylglutaryl-CoA reductase (*HMGCR*) and lanosterol synthase (*LSS*) were numerically decreased (Figure 4, *E* to *H*). For the hypoxia-related genes carbonic anhydrase 9 (*CA9*) and transforming growth factor-β induced protein (*TGFBI*), the P group showed significant suppression, but the B group did not demonstrate suppression (Figure 4, *I* and *J*). Furthermore, expression of *CA9* (22% expression vs. control; $P < .01$) and *TGFBI* (11% expression vs. control; $P < .01$) were significantly reduced compared with control using PB (Figure 4, *K* and *L*). In the BP group the expression of all studied genes was reduced, but none of the reductions were statistically significant. Although transcriptome analysis (LIM1215[A]) had indicated an increase in lipid metabolism pathways in the BB group, quantitative PCR (LIM1215[B]) did not demonstrate enhanced expression of lipogenic genes in this treatment group.

Discussion

Anti-EGFR antibodies and anti-VEGF antibodies represent the current standard of care for front-line mCRC treatment when used in combination with cytotoxic chemotherapy regimens [2,3]; however, evidence suggests that the sequence in which these agents are given to patients may affect clinical outcomes [18–27]. In this study, using xenograft models of *RAS/BRAF* WT CRC, PB was found to be the most

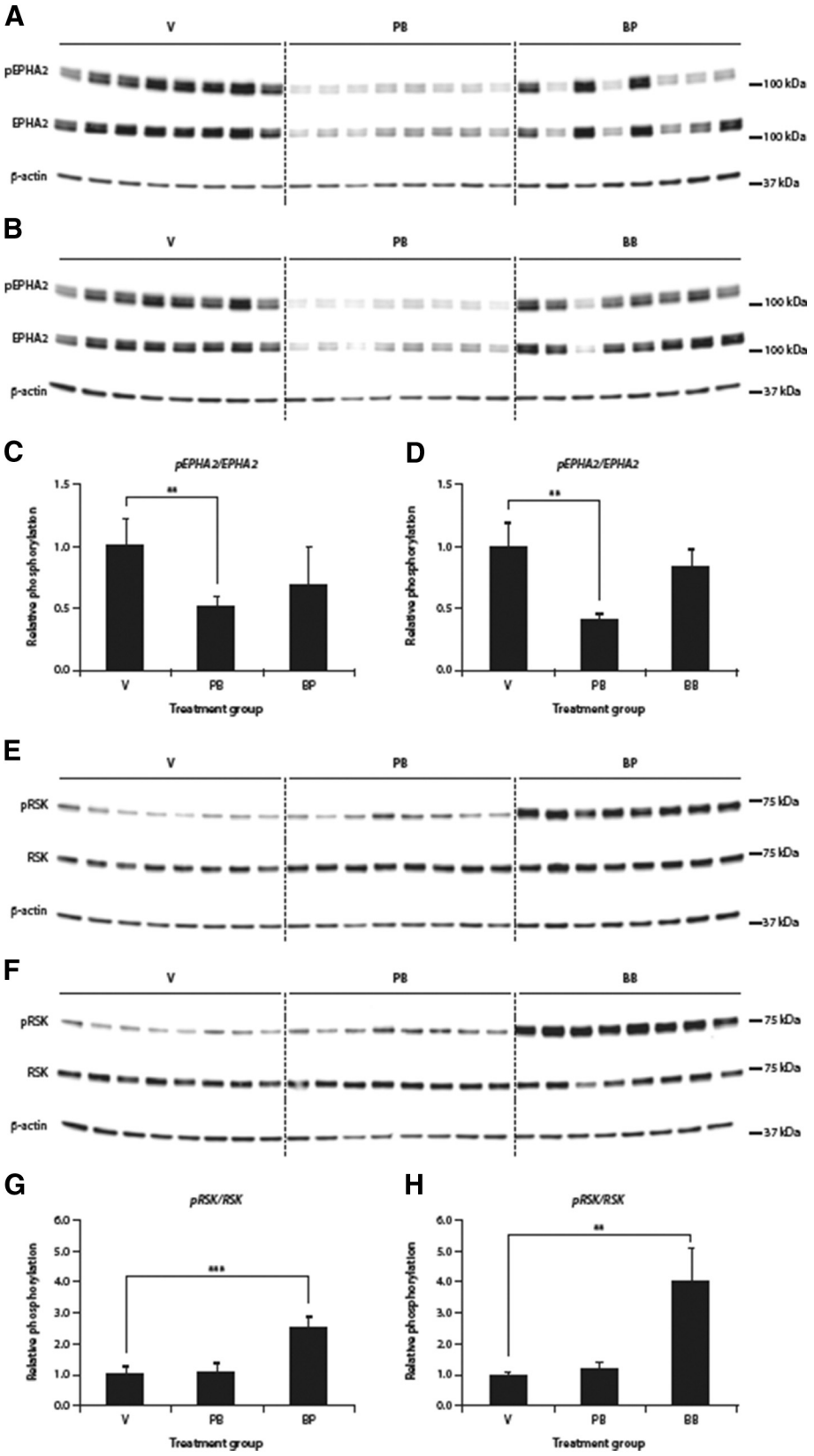

Figure 3. Results of western blotting in LIM1215(B) xenografts. (A) EPHA2 and pEPHA2 with panitumumab-bevacizumab compared with bevacizumab-panitumumab. (B) EPHA2 and pEPHA2 with panitumumab-bevacizumab compared with bevacizumab-bevacizumab. (C) Phosphorylation of EPHA2 for panitumumab-bevacizumab compared with bevacizumab-panitumumab and (D) compared with bevacizumab-bevacizumab. (E) RSK and pRSK with panitumumab-bevacizumab compared with bevacizumab-panitumumab and (F) RSK and pRSK with panitumumab-bevacizumab compared with bevacizumab-bevacizumab. (G) Phosphorylation of RSK for panitumumab-bevacizumab compared with bevacizumab-panitumumab and (H) compared with bevacizumab-bevacizumab. Data represent mean ± SD ($n = 8$). $^{**}P < .01$, $^{***}P < .001$. B, bevacizumab; P, panitumumab; V, vehicle control.

Table 2. Enrichment Analysis of LIM1215(A) Xenografts Treated with Bevacizumab-Bevacizumab Compared with Vehicle Control (all Canonical Pathways, $P < .001$)

Canonical Pathways	*P*-Value
Superpathway of cholesterol biosynthesis	1.3E-18
Cholesterol biosynthesis I	3.2E-12
Cholesterol biosynthesis II (via 24,25-dihydrolanosterol)	3.2E-12
Cholesterol biosynthesis III (via Desmosterol)	3.2E-12
Mevalonate pathway I	3.8E-08
Superpathway of Geranylgeranyldiphosphate biosynthesis I (via Mevalonate)	1.8E-07
Gamma-linolenate biosynthesis II (Animals)	8.7E-06
LXR/RXR activation	5.5E-05
Epoxysqualene biosynthesis	6.3E-05
LPS/IL-1 mediated inhibition of RXR function	7.8E-05
Fatty acid activation	1.3E-04
Stearate biosynthesis I (Animals)	3.2E-04
Mitochondrial L-carnitine shuttle pathway	3.2E-04
FXR/RXR activation	5.4E-04

efficacious treatment sequence with regards to relative GR and reducing the Ki-67 index of tumor cells; the opposite sequence failed to achieve significant reduction of Ki-67 index. Phosphoproteomic analysis also showed that PB was the more effective treatment sequence with regards to reducing the phosphorylation status of key cancer-related signaling proteins, including EGFR and EPHA2, with 36% EPHA2(pS897) phosphorylation with PB versus vehicle control. Western blot experiments confirmed that overall EPHA2 levels and the pEPHA2: EPHA2 ratio were significantly reduced with PB, but not BP or BB, which indicates that PB reduces the phosphorylation status of EPHA2 by mechanisms other than reduction of overall EPHA2 levels.

In this study, the effect of BP could be influenced by the negative impact of bevacizumab on subsequent anti-EGFR efficacy in mCRC, as previously demonstrated in retrospective clinical studies [24–27]. Derangère et al. demonstrated a significant PFS advantage for patients with *RAS* WT mCRC receiving second- or third-line anti-EGFR antibodies after non-bevacizumab therapy compared with prior bevacizumab (4.0 vs. 2.8 months; $P = .003$) [24]. Similarly, a study of patients with *KRAS* exon 2 WT mCRC undergoing anti-EGFR therapy following failure of fluoropyrimidines, oxaliplatin, and irinotecan demonstrated significantly longer PFS and OS and improved response rates for patients who had received bevacizumab more than 6 months prior to anti-EGFR therapy compared with less than 6 months before (PFS 6.6 vs. 4.2 months, $P = .038$; OS 14.3 vs. 11.6 months, $P = .039$; response rate 47.5% vs. 24.3%, $P = .012$) [27]. While such retrospective studies require validation in prospective settings, the findings are consistent with those of the current study.

Treatment with bevacizumab enhances *VEGFA* gene expression in CRC tumors and subsequently increases VEGF-A protein concentrations in the blood [24,28], which in turn is suggested to cause resistance to anti-EGFR antibodies [24]. Similarly, a study using SUM149 xenografts identified a significant reduction in the targeting of radiolabeled cetuximab to tumors following bevacizumab treatment [35]. Alongside our findings, and considering the shared molecular target of cetuximab and panitumumab, such studies suggest biologic mechanisms that may account for the reduced clinical efficacy of anti-EGFR antibodies when administered following an anti-VEGF antibody in mCRC.

Panitumumab suppresses EGFR signaling, preventing transcriptional activation of EPHA2 through MAPK signaling [36,37]. This may explain both the significant reduction in Ki-67 index and reduced expression of EPHA2 that we identified with PB versus vehicle controls. Increased EPHA2 expression in CRC predicts poor response to cetuximab [38,39]. Moreover, S897 phosphorylation of EPHA2 can be induced in a ligand-independent manner by RSK [32–34], Akt [40] or PKA [41]. BP and BB increased RSK phosphorylation compared with vehicle controls; this may be related to the hypoxic response following inhibition of angiogenesis by bevacizumab [42] and subsequent induction of RSK hyperphosphorylation [43].

In terms of gene expression, PB was the only treatment sequence to induce statistically significant reductions in both lipogenic and hypoxia-related genes in our xenograft models (LIM1215[B]). Moreover, changes in the lipogenic genes *FASN, HMGCR*, *MVD*, and *LSS* were also demonstrated in this study. Significant suppression of *FASN* and *MVD* expression was observed with PB, which may indicate anti-tumor activity; reduced activity of lipogenic pathways is suggested to reduce malignancy and suppress oncogenic proliferation [44]. Inhibition of EGFR signaling by panitumumab may lead to functional inhibition of sterol regulatory element binding proteins, thereby reducing expression of lipogenic genes [45,46]. Given that hypoxia is known to induce the expression of lipogenic genes [47], the expression of the hypoxia-related genes *TGFBI* and *CA9* was examined. PB significantly reduced the expression of *CA9* and *TGFBI*, indicative of reduced hypoxic response in the tumor environment. Without therapeutic intervention, hypoxia-inducible factor-1 (HIF-1) is constantly induced in hypoxic tumors and promotes malignant processes. The demonstrated reduction in *CA9* expression is thought to be due to panitumumab-mediated suppression of HIF-1 transcriptional activity or HIF-1 protein expression [48–50]. TGFBI protein is another prognostic factor in CRC [51] thought to be involved in activation of cell proliferation, adhesion, migration, and invasion [52–55]. Therefore, reduced *TGFBI* expression, as demonstrated by PB in the current study, may contribute to the suppression of tumor progression in the clinic.

When interpreting our results, we must consider the limitations associated with the use of xenograft models of human cancers, including the inability of these models to recapitulate the complexity of human cancer [56]. In particular, heterotopic xenograft models, as used in the current study, cannot reproduce the complex tumor-stroma interactions of human autochthonous colorectal carcinoma. Furthermore, xenograft tumors lack the heterogeneity of human tumors due to their construction from standardized cell lines, and tumor interactions with the immune system are compromised in SCID mice. There are also key experimental design factors that differ between studies of xenograft models and cancer in the clinical setting, including the time scales over which the tumor develops and is treated. Consequently, xenograft models in the current study did not become resistant to first-line therapies as would be expected in the clinic; the two-week experimental period was not sufficient to show resistance. Also, other potential factors contributing to anti-EGFR therapy resistance, such as protein levels of VEGF ligands and their receptor [24,28,29], were not monitored in the current study; *VEGFA* mRNA did not change in our transcriptome data, and phosphoproteomic analysis could not detect VEGF-A and VEGFR peptides (data not shown).

In summary, PB has improved activity versus BP in terms of inhibition of tumor growth, reduction of tumor cell proliferation index, reduced expression and phosphorylation status of EPHA2, and down-regulation of expression of lipogenic and hypoxia-related genes. Taken together, these findings may explain in part the reason for the survival benefits previously demonstrated in the clinical settings for the use of first-line anti-EGFR antibodies followed by anti-VEGF antibodies compared with first-line anti-VEGF antibodies followed by anti-EGFR antibodies [19–21].

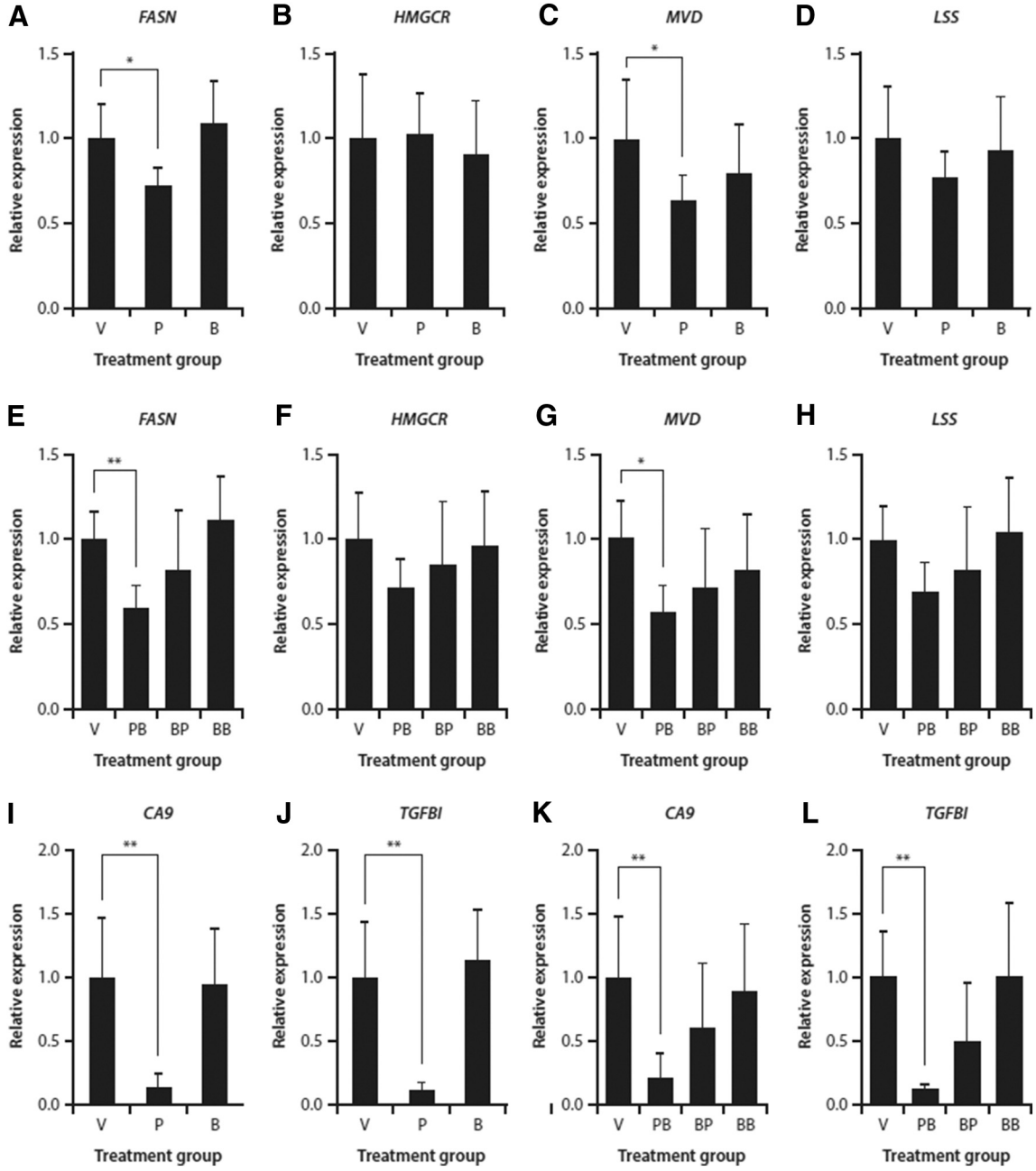

Figure 4. Relative expression of (A–H) lipogenic (*FASN, HMGCR, MVD, LSS*) and (I–L) hypoxia-related (*CA9, TGFBI*) genes in LIM1215(B) xenograft tumors. Expression relative to vehicle control with first-line treatment is shown in (A–D) and (I–J), and with sequential treatment in (E–H) and (K–L). Data represent mean ± SD ($n = 8$). *$P < .05$, **$P < .01$. B, bevacizumab; P, panitumumab; V, vehicle control.

Supplementary data to this article can be found online at https://doi.org/10.1016/j.neo.2018.04.006.

Acknowledgements

Writing assistance for this manuscript was provided by Matthew Hallam, of FireKite, an Ashfield company, part of UDG Healthcare plc, which was funded by Takeda Pharmaceutical Company Limited in compliance with Good Publication Practice 3 ethical guidelines (Battisti et al. Ann Intern Med 2015; 163:461–4).

Experimental support was provided by Akio Mizutani and Yoshihiko Satoh of Pharmaceutical Research Division, Takeda Pharmaceutical Company Limited, and Yasuko Tsuchiya, Asako Tagashira, Saomi Murai, Tadahiro Nambu, Ryo Fukuda and Kotaro Yokoyama of Axcelead Drug Discovery Partners Inc.

Assistance with preparation of this manuscript was provided by Miki Kikko, Yumi Oomuku and Tsuyoshi Osaka of Japan Medical Affairs, Japan Oncology Business Unit, Takeda Pharmaceutical Company Limited.

Conflicts of Interest

H. T. has received financial support for research and lecture fees from Takeda Pharmaceuticals Co. Ltd. and has received lecture fees from Chugai Pharmaceuticals Co. Ltd. and Merck Serono Ltd. Y. B., Y. S., M. G., K. N., H. S., K. Y., Y. S., I. M., Y. H., and J. S. are

employees of Takeda Pharmaceuticals Co. Ltd. H. B. has received financial support for research and lecture fees by Takeda Pharmaceuticals Co. Ltd. and Chugai Pharmaceuticals Co. Ltd.

Funding

This work was funded by Takeda Pharmaceutical Company Limited.

References

[1] Ferlay J, Soerjomatarm I, Ervik M, Dikshit R, Eser S, Mathers C, Rebelo M, Parkin D, Forman D, and Bray F (2014). Cancer Incidence and Mortality Worldwide: IARC CancerBase No. 11 [Internet]. GLOBOCAN 2012 v11. Lyon, France: International Agency for Research on Cancer; 2014 [Available from: http://globocan.iarc.fr, accessed on 30/08/2017].

[2] Van Cutsem E, Cervantes A, Nordlinger B, and Arnold D (2014). Metastatic colorectal cancer: ESMO Clinical Practice Guidelines for diagnosis, treatment and follow-up. *Ann Oncol* **25**(Suppl. 3), iii1–9.

[3] Fakih MG (2015). Metastatic colorectal cancer: current state and future directions. *J Clin Oncol* **33**, 1809–1824.

[4] Bennouna J, Sastre J, Arnold D, Osterlund P, Greil R, Van Cutsem E, von Moos R, Vieitez JM, Bouche O, and Borg C, et al (2013). Continuation of bevacizumab after first progression in metastatic colorectal cancer (ML18147): a randomised phase 3 trial. *Lancet Oncol* **14**, 29–37.

[5] Bokemeyer C, Van Cutsem E, Rougier P, Ciardiello F, Heeger S, Schlichting M, Celik I, and Kohne CH (2012). Addition of cetuximab to chemotherapy as first-line treatment for KRAS wild-type metastatic colorectal cancer: pooled analysis of the CRYSTAL and OPUS randomised clinical trials. *Eur J Cancer* **48**, 1466–1475.

[6] Cunningham D, Lang I, Marcuello E, Lorusso V, Ocvirk J, Shin DB, Jonker D, Osborne S, Andre N, and Waterkamp D, et al (2013). Bevacizumab plus capecitabine versus capecitabine alone in elderly patients with previously untreated metastatic colorectal cancer (AVEX): an open-label, randomised phase 3 trial. *Lancet Oncol* **14**, 1077–1085.

[7] Douillard JY, Oliner KS, Siena S, Tabernero J, Burkes R, Barugel M, Humblet Y, Bodoky G, Cunningham D, and Jassem J, et al (2013). Panitumumab-FOLFOX4 treatment and RAS mutations in colorectal cancer. *N Engl J Med* **369**, 1023–1034.

[8] Hu W, Xu WS, Liao XF, and He HJ (2015). Bevacizumab in combination with first-line chemotherapy in patients with metastatic colorectal cancer: a meta-analysis. *Minerva Chir* **70**, 451–458.

[9] Peeters M, Oliner KS, Price TJ, Cervantes A, Sobrero AF, Ducreux M, Hotko Y, Andre T, Chan E, and Lordick F, et al (2015). Analysis of KRAS/NRAS mutations in a phase III study of panitumumab with FOLFIRI compared with FOLFIRI alone as second-line treatment for metastatic colorectal cancer. *Clin Cancer Res* **21**, 5469–5479.

[10] Cox AD, Fesik SW, Kimmelman AC, Luo J, and Der CJ (2014). Drugging the undruggable RAS: Mission possible? *Nat Rev Drug Discov* **13**, 828–851.

[11] Peeters M, Kafatos G, Taylor A, Gastanaga VM, Oliner KS, Hechmati G, Terwey JH, and van Krieken JH (2015). Prevalence of RAS mutations and individual variation patterns among patients with metastatic colorectal cancer: A pooled analysis of randomised controlled trials. *Eur J Cancer* **51**, 1704–1713.

[12] Hanahan D and Weinberg RA (2011). Hallmarks of cancer: the next generation. *Cell* **144**, 646–674.

[13] Goel S, Huang J, and Klampfer L (2015). K-Ras, intestinal homeostasis and colon cancer. *Curr Clin Pharmacol* **10**, 73–81.

[14] Zhao B, Wang L, Qiu H, Zhang M, Sun L, Peng P, Yu Q, and Yuan X (2017). Mechanisms of resistance to anti-EGFR therapy in colorectal cancer. *Oncotarget* **8**, 3980–4000.

[15] Therkildsen C, Bergmann TK, Henrichsen-Schnack T, Ladelund S, and Nilbert M (2014). The predictive value of KRAS, NRAS, BRAF, PIK3CA and PTEN for anti-EGFR treatment in metastatic colorectal cancer: A systematic review and meta-analysis. *Acta Oncol* **53**, 852–864.

[16] Van Cutsem E, Lenz HJ, Kohne CH, Heinemann V, Tejpar S, Melezinek I, Beier F, Stroh C, Rougier P, and van Krieken JH, et al (2015). Fluorouracil, leucovorin, and irinotecan plus cetuximab treatment and RAS mutations in colorectal cancer. *J Clin Oncol* **33**, 692–700.

[17] Stintzing S, Modest DP, Rossius L, Lerch MM, von Weikersthal LF, Decker T, Kiani A, Vehling-Kaiser U, Al-Batran SE, and Heintges T, et al (2016). FOLFIRI plus cetuximab versus FOLFIRI plus bevacizumab for metastatic colorectal cancer (FIRE-3): a post-hoc analysis of tumour dynamics in the final RAS wild-type subgroup of this randomised open-label phase 3 trial. *Lancet Oncol* **17**, 1426–1434.

[18] Modest DP, Stintzing S, von Weikersthal LF, Decker T, Kiani A, Vehling-Kaiser U, Al-Batran SE, Heintges T, Lerchenmuller C, and Kahl C, et al (2015). Impact of subsequent therapies on outcome of the FIRE-3/AIO KRK0306 trial: First-line therapy with FOLFIRI plus cetuximab or bevacizumab in patients with KRAS wild-type tumors in metastatic colorectal cancer. *J Clin Oncol* **33**, 3718–3726.

[19] Zaniboni A and Formica V (2016). The Best. First. Anti-EGFR before anti-VEGF, in the first-line treatment of RAS wild-type metastatic colorectal cancer: from bench to bedside. *Cancer Chemother Pharmacol* **78**, 233–244.

[20] Wainberg ZA and Drakaki A (2015). The importance of optimal drug sequencing in metastatic colorectal cancer: biological rationales for the observed survival benefit conferred by first-line treatment with EGFR inhibitors. *Expert Opin Biol Ther* **15**, 1205–1220.

[21] Peeters M, Forget F, Karthaus M, Valladares-Ayerbes M, Zaniboni A, Demonty G, Guan X, and Rivera F (2018). Exploratory pooled analysis evaluating the effect of sequence of biological therapies on overall survival in patients with *RAS* wild-type metastatic colorectal carcinoma. *ESMO Open*, **3**e000297.

[22] Lam KO, Lee VH, Liu RK, Leung TW, and Kwong DL (2013). Bevacizumab-containing regimens after cetuximab failure in Kras wild-type metastatic colorectal carcinoma. *Oncol Lett* **5**, 637–640.

[23] Hasegawa H, Taniguchi H, Mitani S, Masuishi T, Komori A, Narita Y, Kadowaki S, Ura T, Ando M, and Yatabe Y, et al (2017). Efficacy of second-line bevacizumab-containing chemotherapy for patients with metastatic colorectal cancer following first-line treatment with an anti-epidermal growth factor receptor antibody. *Oncology* **92**, 205–212.

[24] Derangere V, Fumet JD, Boidot R, Bengrine L, Limagne E, Chevriaux A, Vincent J, Ladoire S, Apetoh L, and Rebe C, et al (2016). Does bevacizumab impact anti-EGFR therapy efficacy in metastatic colorectal cancer? *Oncotarget* **7**, 9309–9321.

[25] Norguet E, Dahan L, Gaudart J, Gasmi M, Ouafik L, and Seitz JF (2011). Cetuximab after bevacizumab in metastatic colorectal cancer: is it the best sequence? *Dig Liver Dis* **43**, 917–919.

[26] Sato Y, Matsusaka S, Suenaga M, Shinozaki E, and Mizunuma N (2015). Cetuximab could be more effective without prior bevacizumab treatment in metastatic colorectal cancer patients. *Onco Targets Ther* **8**, 3329–3336.

[27] Taniguchi H, Komori A, Narita Y, Kadowaki S, Ura T, Andoh M, Yatabe Y, Komori K, Kimura K, and Kinoshita T, et al (2016). A short interval between bevacizumab and anti-epithelial growth factor receptor therapy interferes with efficacy of subsequent anti-EGFR therapy for refractory colorectal cancer. *Jpn J Clin Oncol* **46**, 228–233.

[28] Baba H, Baba Y, Uemoto S, Yoshida K, Saiura A, Watanabe M, Maehara Y, Oki E, Ikeda Y, and Matsuda H, et al (2015). Changes in expression levels of ERCC1, DPYD, and VEGFA mRNA after first-line chemotherapy of metastatic colorectal cancer: results of a multicenter study. *Oncotarget* **6**, 34004–34013.

[29] Viloria-Petit A, Crombet T, Jothy S, Hicklin D, Bohlen P, Schlaeppi JM, Rak J, and Kerbel RS (2001). Acquired resistance to the antitumor effect of epidermal growth factor receptor-blocking antibodies in vivo: a role for altered tumor angiogenesis. *Cancer Res* **61**, 5090–5101.

[30] Greening DW, Lee ST, Ji H, Simpson RJ, Rigopoulos A, Murone C, Fang C, Gong S, O'Keefe G, and Scott AM (2015). Molecular profiling of cetuximab and bevacizumab treatment of colorectal tumours reveals perturbations in metabolic and hypoxic response pathways. *Oncotarget* **6**, 38166–38180.

[31] Wisniewski JR, Zougman A, Nagaraj N, and Mann M (2009). Universal sample preparation method for proteome analysis. *Nat Methods* **6**, 359–362.

[32] Hamaoka Y, Negishi M, and Katoh H (2016). EphA2 is a key effector of the MEK/ERK/RSK pathway regulating glioblastoma cell proliferation. *Cell Signal* **28**, 937–945.

[33] Zhou Y, Yamada N, Tanaka T, Hori T, Yokoyama S, Hayakawa Y, Yano S, Fukuoka J, Koizumi K, and Saiki I, et al (2015). Crucial roles of RSK in cell motility by catalysing serine phosphorylation of EphA2. *Nat Commun* **6**, 7679. https://doi.org/10.1038/ncomms8679.

[34] Graves PR, Din SU, Ashamalla M, Ashamalla H, Gilbert TSK, and Graves LM (2017). Ionizing radiation induces EphA2 S897 phosphorylation in a MEK/ERK/RSK-dependent manner. *Int J Radiat Biol* **93**, 929–936.

[35] Heskamp S, Boerman OC, Molkenboer-Kuenen JD, Oyen WJ, van der Graaf WT, and van Laarhoven HW (2013). Bevacizumab reduces tumor targeting of antiepidermal growth factor and anti-insulin-like growth factor 1 receptor antibodies. *Int J Cancer* **133**, 307–314.

[36] Macrae M, Neve RM, Rodriguez-Viciana P, Haqq C, Yeh J, Chen C, Gray JW, and McCormick F (2005). A conditional feedback loop regulates Ras activity through EphA2. *Cancer Cell* **8**, 111–118.

[37] Pratt RL and Kinch MS (2003). Ligand binding up-regulates EphA2 messenger RNA through the mitogen-activated protein/extracellular signal-regulated kinase pathway. *Mol Cancer Res* **1**, 1070–1076.

[38] Cardone C, Paul MC, Moreno-Viedma V, Martini G, Vitiello PP, Ciardiello D, Sforza V, Troiani T, Napolitano S, and Vitale P, et al (2017). EphA2 expression is a predictive biomarker of poorer activity and efficacy of FOLFIRI + cetuximab in RAS WT metastatis colorectal cancer (mCRC) patients (pts) in the CAPRI-GOIM trial. *Ann Oncol* **28** [abst 1637P].

[39] De Robertis M, Loiacono L, Fusilli C, Poeta ML, Mazza T, Sanchez M, Marchionni L, Signori E, Lamorte G, and Vescovi AL, et al (2017). Dysregulation of EGFR pathway in EphA2 cell subpopulation significantly associates with poor prognosis in colorectal cancer. *Clin Cancer Res* **23**, 159–170.

[40] Miao H, Li DQ, Mukherjee A, Guo H, Petty A, Cutter J, Basilion JP, Sedor J, Wu J, and Danielpour D, et al (2009). EphA2 mediates ligand-dependent inhibition and ligand-independent promotion of cell migration and invasion via a reciprocal regulatory loop with Akt. *Cancer Cell* **16**, 9–20.

[41] Barquilla A, Lamberto I, Noberini R, Heynen-Genel S, Brill LM, and Pasquale EB (2016). Protein kinase A can block EphA2 receptor-mediated cell repulsion by increasing EphA2 S897 phosphorylation. *Mol Biol Cell* **27**, 2757–2770.

[42] Selvakumaran M, Yao KS, Feldman MD, and O'Dwyer PJ (2008). Antitumor effect of the angiogenesis inhibitor bevacizumab is dependent on susceptibility of tumors to hypoxia-induced apoptosis. *Biochem Pharmacol* **75**, 627–638.

[43] Lucien F, Brochu-Gaudreau K, Arsenault D, Harper K, and Dubois CM (2011). Hypoxia-induced invadopodia formation involves activation of NHE-1 by the p90 ribosomal S6 kinase (p90RSK). *PLoS One* **6**e28851.

[44] Baenke F, Peck B, Miess H, and Schulze A (2013). Hooked on fat: the role of lipid synthesis in cancer metabolism and tumour development. *Dis Model Mech* **6**, 1353–1363.

[45] Cheng C, Ru P, Geng F, Liu J, Yoo JY, Wu X, Cheng X, Euthine V, Hu P, and Guo JY, et al (2015). Glucose-mediated N-glycosylation of SCAP Is essential for SREBP-1 activation and tumor growth. *Cancer Cell* **28**, 569–581.

[46] Swinnen JV, Heemers H, Deboel L, Foufelle F, Heyns W, and Verhoeven G (2000). Stimulation of tumor-associated fatty acid synthase expression by growth factor activation of the sterol regulatory element-binding protein pathway. *Oncogene* **19**, 5173–5181.

[47] Furuta E, Pai SK, Zhan R, Bandyopadhyay S, Watabe M, Mo YY, Hirota S, Hosobe S, Tsukada T, and Miura K, et al (2008). Fatty acid synthase gene is up-regulated by hypoxia via activation of Akt and sterol regulatory element binding protein-1. *Cancer Res* **68**, 1003–1011.

[48] Jiang BH, Jiang G, Zheng JZ, Lu Z, Hunter T, and Vogt PK (2001). Phosphatidylinositol 3-kinase signaling controls levels of hypoxia-inducible factor 1. *Cell Growth Differ* **12**, 363–369.

[49] Luwor RB, Lu Y, Li X, Mendelsohn J, and Fan Z (2005). The antiepidermal growth factor receptor monoclonal antibody cetuximab/C225 reduces hypoxia-inducible factor-1 alpha, leading to transcriptional inhibition of vascular endothelial growth factor expression. *Oncogene* **24**, 4433–4441.

[50] Sang N, Stiehl DP, Bohensky J, Leshchinsky I, Srinivas V, and Caro J (2003). MAPK signaling up-regulates the activity of hypoxia-inducible factors by its effects on p300. *J Biol Chem* **278**, 14013–14019.

[51] Zhu J, Chen X, Liao Z, He C, and Hu X (2015). TGFBI protein high expression predicts poor prognosis in colorectal cancer patients. *Int J Clin Exp Pathol* **8**, 702–710.

[52] Thapa N, Lee BH, and Kim IS (2007). TGFBIp/betaig-h3 protein: a versatile matrix molecule induced by TGF-beta. *Int J Biochem Cell Biol* **39**, 2183–2194.

[53] Bae JS, Lee SH, Kim JE, Choi JY, Park RW, Yong Park J, Park HS, Sohn YS, Lee DS, and Bae Lee E, et al (2002). Betaig-h3 supports keratinocyte adhesion, migration, and proliferation through alpha3beta1 integrin. *Biochem Biophys Res Commun* **294**, 940–948.

[54] Kim JE, Jeong HW, Nam JO, Lee BH, Choi JY, Park RW, Park JY, and Kim IS (2002). Identification of motifs in the fasciclin domains of the transforming growth factor-beta-induced matrix protein betaig-h3 that interact with the alphavbeta5 integrin. *J Biol Chem* **277**, 46159–46165.

[55] Shang D, Liu Y, Yang P, Chen Y, and Tian Y (2012). TGFBI-promoted adhesion, migration and invasion of human renal cell carcinoma depends on inactivation of von Hippel-Lindau tumor suppressor. *Urology* **79**, 966.e1–966.e7.

[56] McIntyre RE, Buczacki SJ, Arends MJ, and Adams DJ (2015). Mouse models of colorectal cancer as preclinical models. *Bioessays* **37**, 909–920.